CHEMISTRY
A European Journal

A Journal of ChemPubSoc Europe

Title: Optical limiting properties of 3,5-dithienylenevinylene BODIPY dyes at 532 nm

Authors: Jessica Harris, Lizhi Gai, Gugu Kubheka, John Mack, Tebello Nyokong, and Zhen Shen

To be cited as: *Chem. Eur. J.* 10.1002/chem.201702503

Link to VoR: http://dx.doi.org/10.1002/chem.201702503

Supported by ACES

WILEY-VCH

Optical limiting properties of 3,5-dithienylenevinylene BODIPY dyes at 532 nm

Jessica Harris,‡[a] Lizhi Gai,‡[b] Gugu Kubheka,[a] John Mack,*[a] Tebello Nyokong[a] and Zhen Shen*[b]

Abstract: The optical limiting properties of a series of near infrared absorbing 3,5-dithienylenevinylene BODIPY dyes (**1**-**3**) that contain donor and acceptor moieties in their π-conjugation systems were studied by using the z-scan technique at 532 nm in the nanosecond pulse range. A strong reverse saturable absorption RSA response was observed when the compounds are embedded into poly(bisphenol carbonate A) polymer thin films, which demonstrates that BODIPY dyes with this type of structure are suitable for use in optical limiting applications.

Introduction

Optical limiting (OL) materials have been the focus of considerable research interest in recent years, since they can provide protection from intense incident laser beams.[1-3] Preparing OL materials for the second harmonic of Nd:YAG lasers at 532 nm has become particularly important in the context of aviation safety where the irresponsible use of laser pens is concerned and in the protection of other sensitive optical devices.[4-7] High transmittance of low-intensity light is required under ambient conditions, along with a significant attenuation of an incident pulsed laser beam.[1-3] This has led to considerable interest in the OL properties of porphyrins,[8,11] phthalocyanines,[8-10] fullerenes,[1] and other organic chromophores,[12,13] nanoparticles,[14] metal nanowires,[15] and carbon nanotubes.[16] The main mechanisms involved in achieving an OL response are nonlinear absorption (NLA), nonlinear refraction (NLR) and nonlinear scattering (NLS).[17,18] In this study, however, the main focus is on the OL properties of molecular dyes that are caused by NLA processes and result in a strong reverse saturable absorption (RSA) response that leads to a decrease in transmittance at high incident light intensity levels.

OL properties often depend on two-photon absorption (2PA), which is a resonant third-order nonlinear optical (NLO) process in which an excited state is formed by the simultaneous absorption of two photons of half-energy, in an intense focused light beam such as that generated by a laser source.[19,20] It has been demonstrated that π-conjugation systems possess large electronic polarizabilities, and hence it is reasonable to expect molecules of this type to possess the substantial second-order hyperpolarizabilities that enhance their OL properties.[21,22] Molecules with donor and acceptor moieties that are separated by a π-conjugation system (D-π-A) are also known to exhibit large third order susceptibility values.[19] In this study, 3,5-dithienylenevinylene BODIPY dyes (**1**-**3**) with electron donating 2-thiophene rings have been studied to assess their potential for OL applications (Scheme 1). To the best of our knowledge, the properties of 3,5-dithienylenevinylene BODIPY dyes have not been studied to any significant extent in the context of OL at 532 nm. BODIPY **3** is also substituted at the 2,6-positions with iodine atoms, since the presence of heavy atoms promotes intersystem crossing from the singlet to the triplet excited state by enhanced spin-orbit coupling and results in a significantly lower fluorescence quantum yield.[23]

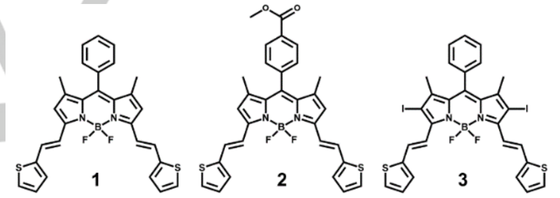

Scheme 1. The BODIPY dyes that were synthesized in this work for NLO studies.

Although the use of optically transparent organic solutions is convenient for investigating the OL properties of dye molecules, for the purpose of applications it is necessary for the OL materials to be cast in the solid state, since incorporation into safety visors or Perspex™ windshields is envisaged. In this work, BODIPYs **1**−**3** were embedded in poly(bisphenol carbonate A) (PBC) polymer thin films,[24,25] since polycarbonates have previously been used for making safety visors,[26] and in the manufacture of eyewear, protective sportswear and other safety products. There have been comparatively few studies on the use of BODIPY dyes and their analogues as OL materials for 532 nm excitation pulses[27-29] and those at other wavelengths.[30-32] This study clearly demonstrates that near infrared absorbing BODIPY dyes with extended D-π-A conjugation structures are potentially suitable for OL applications.

Results and Discussion

Synthesis and Characterization: BODIPYs are conventionally prepared through an acid-catalyzed condensation reaction of a pyrrole ring with an aromatic aldehyde.[33] 2,4-dimethylpyrrole is usually preferred as a starting material, since the methyl-substituents prevent the formation of porphyrins. The 1,3,5,7-tetramethylBODIPYs that are formed in this manner can be

---

[a] Dr. J. Mack, J. Harris, G. Kubheka, Prof. T. Nyokong
Department of Chemistry
Rhodes University
Grahamstown 6410 (South Africa)
E-mail: j.mack@ru.ac.za
[b] Prof. Zhen Shen, L. Gai
State Key Laboratory of Coordination Chemistry
Nanjing National Laboratory of Microstructures
Nanjing University; Nanjing 210023 (P.R. China)
E-mail: zshen@nju.edu.cn

‡ These authors contributed equally to this work.
Supporting information for this article is given via a link at the end of the document.

10.1002/chem.201702503

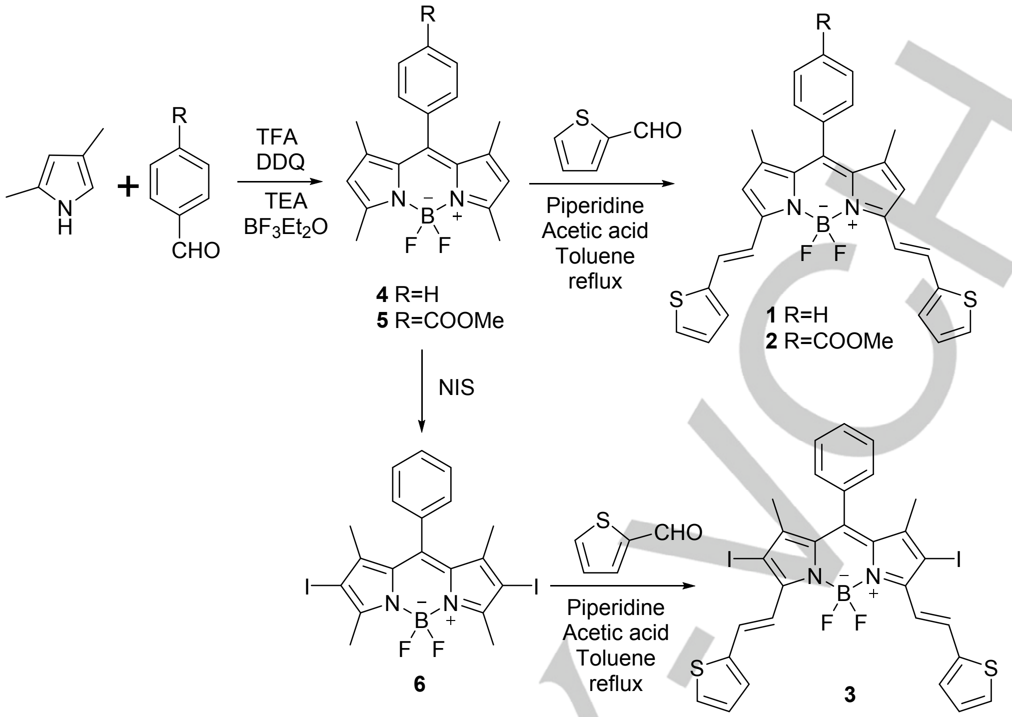

Scheme 2. The BODIPY dyes that were synthesized in this work for NLO studies.

readily iodinated at the 2,6-positions with N-iodosuccinimide (NIS). The introduction of vinyl groups was achieved by reacting an aromatic aldehyde with the appropriate 2,6-dibromoBODIPY to form (Scheme 2).[34,35] The introduction of vinyl groups is one of the most useful strategies for shifting the main spectral band of the BODIPY chromophore to the red (Figure 1).[36] The protons attached to the methyl groups are acidic enough to undergo condensation reactions. Extension of the π-conjugation and the addition of functionality is most frequently accomplished through the methyl groups at the 3,5-positions, since this generally produces a greater red shift (ca. 50−100 nm) than is observed upon extending the π-conjugation through the 2,6-[26] or 1,7-positions.[37] The main spectral bands of **1** and **2** lie at ca. 650 nm (Table 1), while iodination results in a further red shift of the main spectral band of **3** to 670 nm. The fluorescence quantum yield (Φ_F) and lifetime values (τ_F) of **3** (Table 1) were found to be significantly lower than those of BODIPYs **1** and **2** due to the presence of iodine atoms at the 2,6-positions, which increases the rate of ISC through a relaxation of the spin-selection rule.

The ground state absorption spectra of the thin films were obtained in order to visualize the effect of a solid support. Figure 1 contains the absorption spectra of **1**-**3** in DMF and embedded in poly(bisphenol A carbonate) (PBC) as thin films (**1**-PBC, **2**-PBC, and **3**-PBC). The DMF spectra show the main absorption bands of the BODIPYs are well defined and do not show signs of aggregation. For BODIPY **1**, the DMF spectrum is well-defined but the **1**-PBC spectrum shows significant aggregation. The thin film spectra of **2** and **3** are slightly red-shifted but show that the BODIPYs maintain their electronic character.

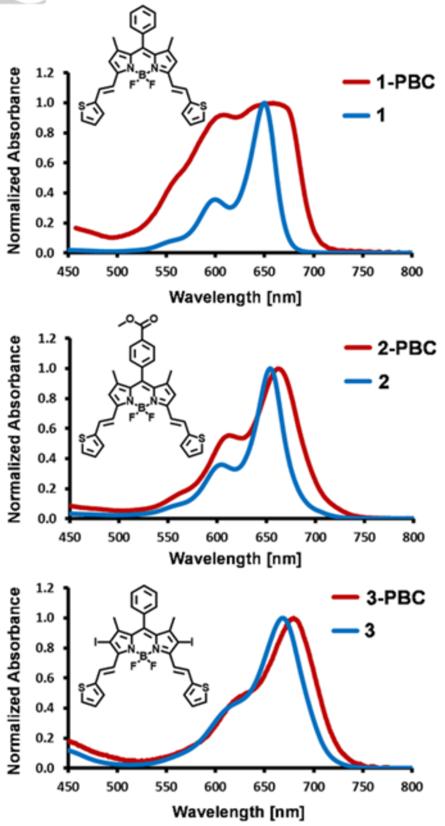

Figure 1. Ground state absorption spectra for BODIPYs **1**-**3** in DMF (blue) and embedded in PBC thin films (red).

Table 1. Photophysical data for 3,5-dithienylenevinylene BODIPYs **1**-**3** in DMF.

	log ε	**λ_{abs} [nm]**	**λ_{exc} [nm]^a**	**λ_{em} [nm]^a**	**Φ_F**	**τ_F [ns]**
1	5.00	651	651	663	0.33	2.89
2	5.05	656	656	671	0.40	2.87
3	4.73	670	670	695	0.11	1.62

[a] Excitation and emission spectra are provided in Figure S1, Supplementary Information.

NLO properties: The measured quantity in an open-aperture z-scan experiment is the normalized transmittance, given by Equation 1 for a Gaussian pulse.[38,39]

$$T(z) = \frac{1}{\sqrt{\pi}q_0(z)}\int_{-\infty}^{\infty}\ln[1 + q_0(z)e^{-\tau^2}]\mathrm{d}\tau \qquad (1)$$

Where $q_0(z)$ is a parameter characterizing the strength of the nonlinearity and is given by Equation 2 when using a circular Gaussian beam.[38,39]

$$q_0(z) = \frac{2\beta P_0 L_{eff}}{\pi w(z)^2} \qquad (2)$$

where β is the nonlinear absorption coefficient of the material, P_0 is the peak power of the pulses and L_{eff} is the effective path length in the sample, given by Equation 3:

$$L_{eff} = \frac{1-e^{-\alpha L}}{\alpha} \qquad (3)$$

where α is the linear absorption coefficient. For applications of these materials, α should always be measured at the intended wavelength:[19] in this case, 532 nm. In Equation 2, $w(z)$ is the beam width as a function of the sample position, and is given by:[19]

$$w(z) = w_0\sqrt{1+\left(\frac{z}{z_0}\right)^2} \qquad (4)$$

where w_0 is the beam waist at the focus (z = 0), defined as the distance from the beam centre to the point where the intensity reduces to $1/e^2$ of its axis value; while z and z_0 are the translation distance of the sample relative to the focus, and Rayleigh length, respectively. The Rayleigh length is defined as $\pi w_0^2/\lambda$ where λ is the wavelength of the laser. Equations 1-4 are used to determine the nonlinear absorption coefficient (β) from experimentally measured normalized transmittance. Tsigaridas et al.[39] have produced an analytical formula given by Equation 5:

$$q_0(z) = \begin{cases} a_0+a_1T(z)+a_2T^2(z)+a_3T^3(z) \text{ for } T(z) \leq 0.75 \\ c_0+c_1[T(z)]^{c_2} \text{ for } T(z) \geq 0.75 \end{cases} \qquad (5)$$

where the coefficients a_0, a_1, a_2, a_3, c_0, c_1 and c_2 for Gaussian pulses are given as 15.66, −37.45, 30.76, −8.97, −2.301, 2.156 and −1.563 respectively.[39] Equation 5 provides values of $q_0(z)$ directly from the normalized transmittance $T(z)$. Substituting Equation 4 into Equation 2 gives $q_0(z)$ as follows:

$$q_0(z) = \frac{Q_0}{1+\left(\frac{z}{z_0}\right)^2} \qquad (6)$$

where

$$Q_0 = \frac{2\beta P_0 L_{eff}}{\pi w_0^2} = \frac{2\beta P_0 L_{eff}}{\lambda z_0} \qquad (7)$$

Equation 5 gives a Gaussian plot with Q_0 as the maximum value at the beam waist (z = 0). The peak value and the FWHM of the plot give values of Q_0 and z_0 respectively. The value of β may then be calculated using Equation 8.[39]

$$\beta = \frac{\lambda z_0 Q_0}{2P_0 L_{eff}} \qquad (8)$$

The imaginary component of the third order susceptibility, Im[$\chi^{(3)}$], is directly proportional to β, as seen in Equation 9:

$$\mathrm{Im}\left[\chi^{(3)}\right] = \frac{\eta^2\varepsilon_0 c\lambda\beta}{2\pi} \qquad (9)$$

where η and c are the linear refractive index and speed of light, respectively, and ε_0 is the permittivity of free space. The third-order nonlinear optical susceptibility is used to describe ultrafast responses,[40] with nonlinear absorption being described by the imaginary component, while the real component is representative of the nonlinear refraction of the material. The optimal range for Im[$\chi^{(3)}$] is 10^{-9}–10^{-11} esu. While Im[$\chi^{(3)}$] describes the speed of the NLA response of the material, the behavior at a molecular level may be described using hyperpolarizability (γ), which describes the nonlinear absorption per mole of the OL compound, and is useful when comparing efficiencies of different optical limiters. The correlation between Im[$\chi^{(3)}$] and γ is shown in Equation 10:

$$\gamma = \frac{\mathrm{Im}[\chi^{(3)}]}{f^4 C_{mol} N_A} \qquad (10)$$

where N_A is Avogadro's constant, C_{mol} is the concentration of the active species in the excited state per mole, and f is the Lorentz local field factor, $f = (\eta^2+2)/3$.[41] Optimal values of γ lie in the 10^{-29}-10^{-34} esu range.

The limiting intensity (I_{lim}) is the threshold fluence value at which the transmittance is 50% of the linear transmittance. It is possible to approximate the value of I_{lim} experimentally, using a plot of output fluence (I_{out}) vs input fluence (I_{in}). While there is currently no defined optimal range for I_{lim} values, it makes sense that a good optical limiter would be those compounds exhibiting lower I_{lim} values, as this means that the limiting would occur at a lower intensity, allowing for more cautious protection of sensors. As a guideline on limits of exposure to radiation, the International Commission on Non-Ionizing Radiation Protection has published a guideline[42] giving insight into exposure limits for a variety of lasers. This work deals with 10 ns pulses of light at 532 nm derived from an Nd:YAG laser through the use of a second harmonic generation crystal and, as such, its exposure limit can be determined from Equation 11, which gives the exposure limit as a function of time.

$$2.7C_A t^{0.75} \text{ Jcm}^{-2} \qquad (11)$$

C_A is a correction factor (= 1 for lasers with wavelengths of 400-700 nm). For this work, the exposure limit (t) was determined to be 0.95 Jcm^{-2} assuming a 0.25 s exposure time. This exposure time was selected because it is the average human response time (blink reflex) to a sudden flux of light into the eye.[43] Irradiance

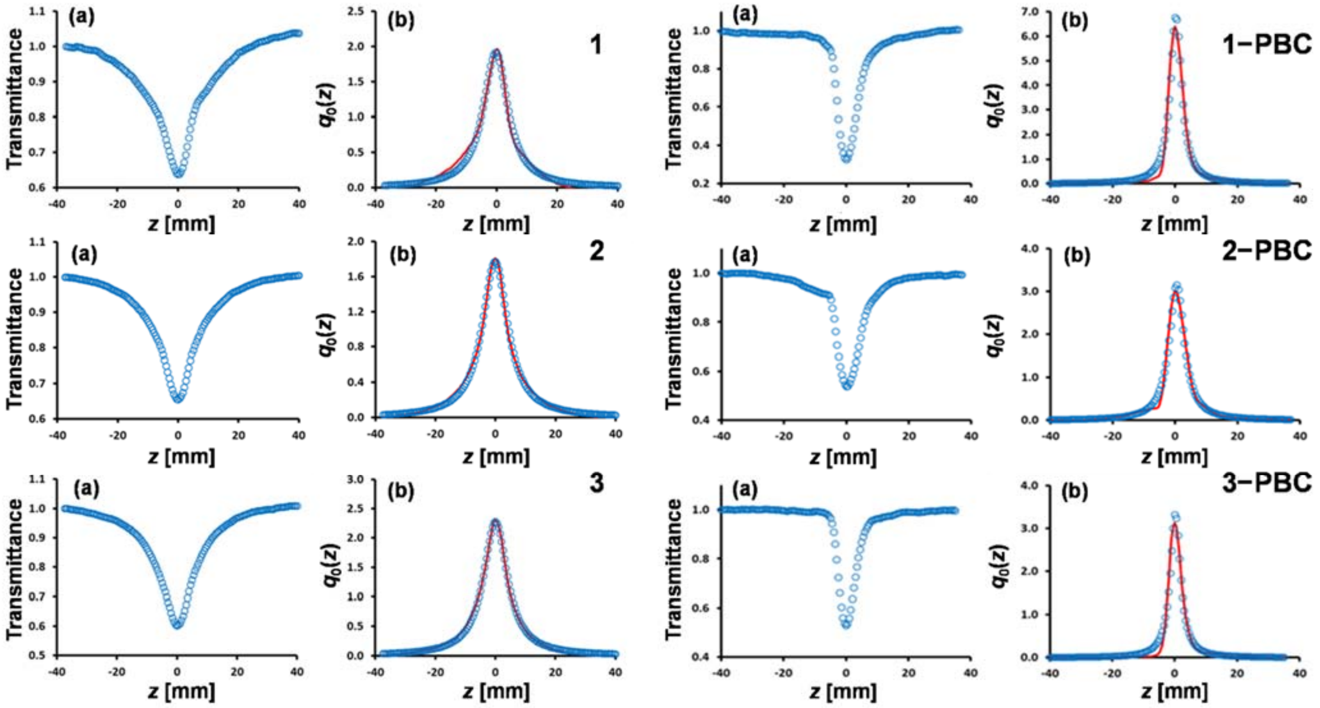

Figure 2. Z-scan (a) and nonlinear fit ($q_0(z)$) curves (b) for BODIPYs **1**-**3** in DMF solution and when embedded in thin films. Detailed NLO parameters are provided in Table 2. Red lines are used to show the response curves that were calculated using Equation 5.

has units of Wcm^{-2}, with the maximum value occurring at the focus (z = 0), determined by Equation 12.

$$I_{00} = \frac{E}{\pi w_0^2} \qquad (12)$$

where E is maximum laser energy (J), τ is the length of the laser pulse (s) and w_0 is beam waist (cm). Since 1 Js^{-1} = 1 W, the maximum irradiance has units of Wcm^{-2}. For any given z-scan experiment, the laser energy remains constant and hence, the overall laser power also remains constant. However, the irradiance varies with z, as the beam width depends on the distance from the focus. The cross-sectional area of the beam is circular and hence equal to $\pi w(z)^2$. Multiplying the irradiance by the corresponding beam area gives the laser power, P. At the focus (z = 0), P is given by Equation 13.

$$P = I_{00}\pi w_0^2 \qquad (13)$$

At any other z position, P is given by Equation 14.

$$P = I_{in}(z)\pi w(z)^2 \qquad (14)$$

As P remains constant throughout any given z-scan run, Equations 13 and 14 can be combined and simplified as shown in Equation 15:

$$I_{in}(z) = I_{00}\left(\frac{w_0}{w(z)}\right)^2 \qquad (15)$$

As the transmittance gives the percentage of light that passes through a material, the output fluence ($I_{out}(z)$) may be calculated by finding the product of $I_{in}(z)$ and the transmittance corresponding to each z position ($T(z)$) (Equation 16).

$$I_{out}(z) = I_{in}(z)\,T(z) \qquad (16)$$

The open aperture z-scan method was used to characterize the OL properties of the series of 3,5-divinyl-BODIPY dyes selected for this study. The β value is an important parameter for assessing the suitability of materials for optical limiting, since it measures the degree of nonlinear absorptivity and depends on the population of molecules in the excited state. Generally, this parameter depends on two-photon absorption processes.[17,44] Since nanosecond pulses are used excited state absorption (ESA) can also happen on this timescale. When the ESA is more intense than the absorption in the ground state, ESA from a two-photon pumped state can also provide the RSA response that is required for optical limiting. These OL mechanisms result in positive nonlinear absorption coefficients, and a decrease in transmittance as the material approaches the zero position of the z-scan instrument at high-intensity levels.[45]

Figures 2-4 show the representative open-aperture z-scans at 532 nm using 10 ns pulses for **1**-**3** in DMF solution and in thin films. The main OL parameters that were calculated on this basis are provided in Table 2. The measurements demonstrate that there is strong nonlinear absorption behavior in both samples, with the shapes of the z-scan profile exhibiting RSA signatures.[46] Analyses of the z-scan results to obtain β_{eff} values were carried out by fitting the data to the 2PA-assisted ESA function described above.

Table 2. Optical limiting properties of **1**-**3** in DMF and in thin films.

	Concentration × 10^{-5} [M][a] Film-thickness [μm][b]	α [cm^{-1}]	β_{eff} × 10^{-9} [mW^{-1}]	Im[$\chi^{(3)}$] × 10^{-10} [esu]	γ [esu]	I_{lim} [Jcm^{-2}]	I_{out} % at 50% I_{in}
1	9.73[a]	0.63	1.40	0.46	1.20 × 10^{-30}	---	80
2	8.56[a]	0.82	1.35	0.44	1.31 × 10^{-30}	---	78
3	18.10[a]	0.88	1.62	0.53	7.58 × 10^{-31}	1.63	71
1-PBC	21[b]	103	21.1	6.89	7.8 × 10^{-29}	0.61	39
2-PBC	21[b]	56	13.0	4.24	4.2 × 10^{-29}	0.40	25
3-PBC	17[b]	12	11.5	3.76	2.5 × 10^{-28}	0.96	38

[a] Concentration in DMF solution. [b] Average thickness of BODIPY-embedded PBC films.

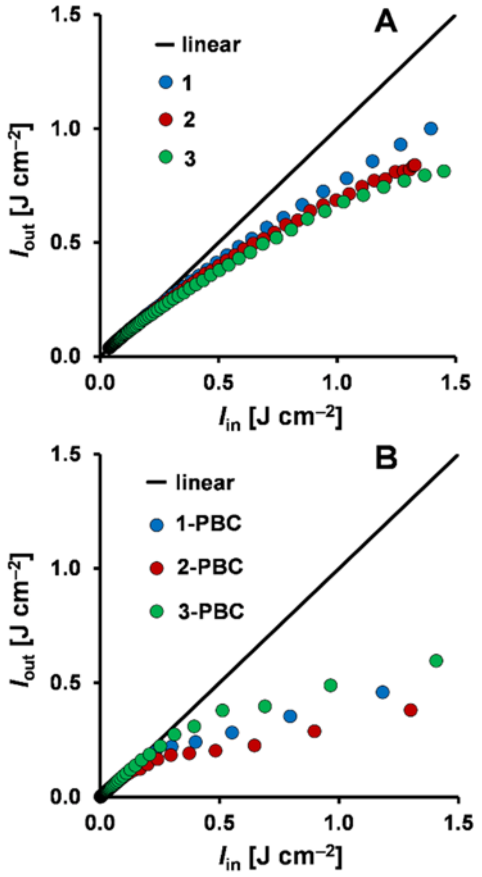

Figure 3. Output fluence (I_{out}) versus input fluence (I_{in}) curves for **1**-**3** in DMF (A) and in thin films (B). Detailed NLO parameters are provided in Table 2.

In molecules where the linear absorption at the laser wavelength of 532 nm is zero, all the observed absorption at that wavelength must be due to multi-photon absorption. However, when nanosecond pulses are used as is the case in this study it may also be due to sequential 2PA and ESA,[27] so the intrinsic value for β that is associated only with 2PA cannot be determined, and an effective value (β_{eff}) is determined instead. Additionally, thiophene-substituted BODIPYs **1**-**3** have a small amount of linear absorbance occurring at 532 nm, which means that the S_1 state can be populated through the absorption of a single photon as well as through 2PA. Thus, there are multiple processes that could be contributing to the OL properties of these compounds. Recently, a styryl-substituted BODIPY,[27] has reportedly shown strong RSA behavior consistent with 2PA-assisted ESA from its longer lived S_1 excited state.[27] The z-scan plots for BODIPYs **1**-**3** in solution are shown in Figure 2. The z-scan plots show a typical nonlinear absorption behavior, with RSA profiles. Equations 1-4 were used to determine the β_{eff} values for each sample, and the results are summarized in Table 2. The experimental β_{eff} values for BODIPYs **1**-**3** in DMF solution were found to be 1.40 × 10^{-9}, 1.35 × 10^{-9}, and 1.62 × 10^{-9} mW^{-1}, respectively. The magnitude of the β_{eff} values for BODIPYs **1**-**3** lie within the range of values previously reported for other organic compounds with promising OL properties.[24]

BODIPYs **1**-**3** were embedded in PBC as thin films and their β values measured. Z-scan plots for the thin films are shown in Figure 2. The β_{eff} values of the **1**-PBC, **2**-PBC and **3**-PBC thin films were found to be 21.1 × 10^{-9}, 13.0 × 10^{-9}, and 11.5 × 10^{-9} mW^{-1}, respectively. The β_{eff} values of **1**-**3** were significantly improved in this context, which has previously been attributed to aggregation of the molecule.[46] The effects of aggregation are noticeable in the spectrum of **1**-PBC (Figure 1), which has significantly higher absorption at 532 nm and more noticeable broadening of the main spectral band in the NIR region, but appear to be relatively minor in the spectra of the **2**-PBC and **3**-PBC thin films.

Table 2 summarizes the third-order nonlinear susceptibility (Im[$\chi^{(3)}$]) and second-order hyperpolarizability values of BODIPYs **1**-**3** in solution and as thin films. The γ value (Table 2) provides a measure of the interaction of an incident photon with the permanent dipole moment of the BODIPY dyes at a molecular level, while the Im[$\chi^{(3)}$] value provides a measure of the ultra-fast response of an NLO material. Since the γ values describe the nonlinear absorption per mole of the OL compound, it is useful when comparing the efficiencies of different optical limiters. Both the Im[$\chi^{(3)}$] and γ values are required to be sufficiently large for a material to be considered promising for OL applications; reported values for Im[$\chi^{(3)}$] and γ are typically in the range of 10^{-9}–10^{-15} and 10^{-29}–10^{-34} esu, respectively.[47] The concentrations of BODIPYs **1**-**3** in solution were determined to be in the order of 10^{-4} M (Table 2), while the thicknesses of the films were determined to be 21 μm for **1**-PBC and **2**-PBC, and 17 μm for **3**-PBC by using scanning electron microscopy (see Figure S2, Supplementary Information). The Im[$\chi^{(3)}$] values obtained for both solutions and thin films lie in the 10^{-9}–10^{-15} range, while the γ values of the **1**-PBC and **2**-PBC thin films also fall within the literature range. The γ value of the 2,6-halogenated BODIPY in the **3**-PBC thin film was even more favorable. In general, the Im[$\chi^{(3)}$] and γ values are much larger in thin films compared to the corresponding solution (Table 2). **1**, which showed a particularly high β_{eff} value in the context of the **1**-PBC thin film, also has a high value for Im[$\chi^{(3)}$] (Table 2), as the two quantities are directly proportional.

10.1002/chem.201702503

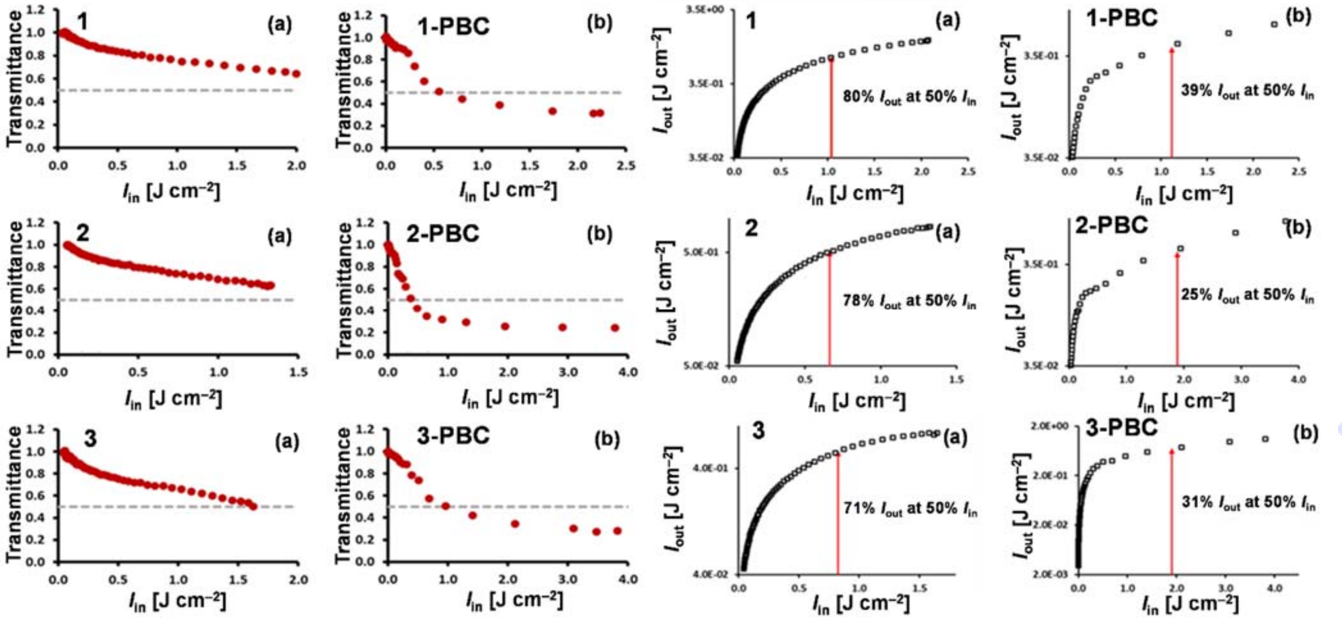

Figure 4. (LEFT) Normalised transmittance vs input fluence curves BODIPYs **1**-**3** in DMF (a) and embedded in PBC as thin films (b). Grey dashed lines indicate 50% transmittance and are used to identify the I_{lim} values. (RIGHT) Logarithmic plot of I_{out} versus I_{in} for BODIPYs **1**-**3** measured in DMF solutions (a) and embedded in PBC as thin films (b). Detailed NLO parameters are provided in Table 2.

The limiting threshold intensity or fluence value, I_{lim}, is defined as the input fluence at which the nonlinear transmittance is 50% of the linear transmittance. The value of I_{lim} can be determined using plots of input fluence vs. output fluence (Figure 3), and transmittance vs. input fluence (Figure 4). The I_{lim} values of **1** and **2** in solution could not be estimated, since the transmittance did not drop below 50% (Figure 4 and Table 2), while that of **3** is 1.63 Jcm^{-2}. The values for the thin films were 0.61, 0.40 and 0.96 Jcm^{-2} for **1**-**3**, respectively. The values for **1**-PBC and **2**-PBC, which contain non-iodinated BODIPYs fall well below the damage threshold of 0.95 Jcm^{-2}, which suggests that the introduction of heavy atoms at the 2,6-positions of the BODIPY core provides no significant advantage in this regard. A logarithmic plot of I_{out} versus I_{in} can also provide a rough comparison of the OL properties of different optical limiting materials. Figure 4 shows the logarithmic plot of I_{out} versus I_{in} for BODIPYs **1**-**3** in DMF and as films. The I_{out} percentage values suggest that the responses of BODIPYs **1** and **2** are very similar (80% and 78%, respectively), while that of BODIPY **3**, which contains iodine atoms at the 2,6-positions, is even better (at 71%). However, **2**-PBC shows a significantly better response of 25%, while **1**-PBC and **3**-PBC have I_{out} percentage values of 40%, and 38%, respectively.

Conclusions

Nanosecond timescale open aperture z-scan studies demonstrate near infrared absorbing BODIPY dyes with D-π-A structures, such as the 3,5-dithienylenevinylene BODIPY dyes in this study, have relatively strong OL properties and relatively weak absorbance under ambient light conditions at an excitation wavelength of 532 nm making dyes of this type potentially suitable for optical limiting applications where the second harmonic of Nd:YAG lasers is concerned. The I_{lim} values for PBC films embedded with **1**-**3** are significantly below the threshold value that has been reported for damage to the human eye of 0.95 Jcm^{-2}. These results demonstrate that BODIPY dyes with D-π-A structures are potentially suitable for use in OL applications, such as use in thin films to enhance aviation safety and protect sensitive optical devices. Further studies are already in progress to determine how the structures of BODIPY dyes can be modified to further enhance the OL properties.

Experimental Section

General: All air and moisture-sensitive reactions were carried out under a nitrogen atmosphere. Poly(bisphenol A carbonate) was obtained from Fluka Analytical (M_W ~ 28,200, *d*: 1.2 g ml^{-1} at 298 K). All other reagents were obtained from commercial suppliers and used without further purification unless otherwise indicated. Dichloromethane was distilled over calcium hydride. Triethylamine was obtained by simple distillation. Ether and THF were distilled over sodium. ^{1}H and ^{13}C NMR spectra were measured by using a Bruker DRX600 spectrometer and referenced to the residual proton signals of the solvent. Mass spectral data were obtained on a Bruker Daltonics AutoflexII™ MALDI-TOF spectrometer. Elemental analyses were carried out using a Vario-Elementar Microcube ELIII Series CHNS analyzer.

Equipment: Electronic absorption spectra were measured on a Shimadzu UV-2550 spectrophotometer. Fluorescence emission spectra were recorded on a Varian Eclipse spectrofluorimeter, while fluorescence lifetimes were measured using a time-correlated single photon counting (TCSPC) spectrometer (FluoTime 200, Picoquant GmbH). A frequencydoubled Quanta-Ray Nd:YAG laser was used as an excitation source for the z-scan measurements in a near-Gaussian transverse mode at 532 nm, and the input and output energies were determined with Coherent J5-09 detectors. A low pulse repetition rate of 10 Hz was used to avoid the occurrence of cumulative thermal nonlinearities. The beam was filtered spatially so that higher order modes can be eliminated before being focussed with a lens (focal length = 15 cm). A 2 mm quartz cuvette was used during the z-scan measurements in DMF solution. The PBC thin film thicknesses were determined using a TESCAN Vega TS 5136LM scanning electron microscopy instrument.

Synthesis: BODIPYs **3**-**6** (Scheme 1) were prepared in a similar manner according to the literature procedures.[48-51]

In a round bottom flask equipped with a Dean-Stark apparatus, a mixture of BODIPY **4** (64 mg, 0.2 mmol), 2-thiophene-carboxaldehyde (40 mg, 0.4 mmol), glacial acetic acid (0.4 mL, 7.0 mmol), and piperidine (0.8 mL, 8 mmol) in toluene (20 mL) was refluxed for 10 h. The solution was heated at reflux for 12 h. After cooling to room temperature, the mixture was washed three times with water. $MgSO_4$ was added to dry the organic phase, and the solvent was evaporated under reduced pressure. The crude residue was purified by silica-gel column chromatography (eluent: hexane/ethyl acetate (10:1)) to afford compound **1** (27.7 mg, 27%). ^1H NMR (600 MHz, [D$_6$]Acetone): δ 7.73 (d, *J* = 16.1 Hz, 2H), 7.67−7.58 (m, 5H), 7.54−7.49 (m, 4H), 7.35 (d, *J* = 3.4 Hz, 2H), 7.20−7.14 (m, 2H), 6.89 (s, 2H), 1.48 (s, 6H) ppm; ^{13}C NMR (150 MHz, [D$_8$]THF): δ 150.25, 141.19, 140.62, 140.61, 136.58, 133.50, 131.47, 127.15, 126.79, 126.72, 126.36, 126.00, 125.10, 116.60, 115.81, 12.01 ppm; MALDI-TOF MS: m/z calcd: 512.45; found: 511.96 [M]$^+$; elemental analysis calcd (%) for $C_{29}H_{23}BF_2N_2S_2$: C 67.97, H 4.52, N 5.47, S 12.51; found: C 67.82, H 4.51, N 5.43, S 12.68.

2 was prepared by following a procedure similar to that used for **1** by using BODIPY **5** and was obtained in 33% yield. ^1H NMR (600 MHz, [D$_6$]Acetone): δ 8.26 (d, *J* = 8.0 Hz, 2H), 7.75 (d, *J* = 16.2 Hz, 2H), 7.69 (d, *J* = 8.1 Hz, 2H), 7.61 (d, *J* = 5.0 Hz, 2H), 7.53 (d, *J* = 16.2 Hz, 2H), 7.36 (d, *J* = 3.4 Hz, 2H), 7.18−7.15 (m, 2H), 6.91 (s, 2H), 3.98 (s, 3H), 1.48 (s, 6H) ppm; ^{13}C NMR (150 MHz, [D$_8$]THF): δ 163.67, 150.53, 140.56, 139.37, 138.17, 135.23, 131.04, 129.07, 128.20, 127.38, 127.13, 126.55, 126.05, 125.28, 116.47, 116.02, 49.53, 12.16 ppm; MALDI-TOF MS: m/z calcd: 570.49; found: 570.10 [M]$^+$; elemental analysis calcd (%) for $C_{31}H_{25}BF_2N_2O_2S_2$: C 65.27, H 4.42, N 4.91, S 11.24; found: C 65.16, H 4.40, N 4.85, S 11.27.

Poly(bisphenol A carbonate) (110 mg) and thiophene-substituted BODIPYs **1**-**3** (0.1 mg) were dissolved in DCM (1.5 mL) and sonicated until a homogeneous mixture of BODIPY-polymer solution was obtained. The BODIPY-PBC solutions were dropped on glass substrates placed in a Petri dish and the solvent was allowed to evaporate at room temperature. The average film thickness was determined to be 21, 21 and 17 μm for **1**-PBC, **2**-PBC, and **3**-PBC, respectively, by using scanning electron microscopy (see Figure S2, Supp. Info.).

Acknowledgements

This study was made possible by support from a China-South Africa joint research program (CS08-L07 and uid: 95421) to ZS and JM, a Competitive Support for Unrated Researchers grant from the National Research Foundation of South Africa (uid: 93627) to JM, Major State Basic Research Development Program of China (Grant Nos. 2013CB922101 & 2011CB808704), the National Natural Science Foundation of China (No. 21371090), and Natural Science Foundation of Jiangsu Province (BK20130054) grants to ZS, and a Pearson Young Memorial Scholarship to JH. Photophysical measurements were made possible by the Laser Rental Pool Programme of the Council for Scientific and Industrial Research (CSIR) of South Africa. The authors thank Marcel Louzada for help with the z-scan calculations.

Keywords: Dyes/Pigments • BODIPYs • nonlinear optics • optical limiting • z-scan

[1] L. W. Tutt, A. Kost, *Nature* **1992**, *356*, 225−226.
[2] J. W. Perry, K. Mansour, I. Y. S. Lee, X. L. Wu, P. V. Bedworth, C. T. Chen, D. Ng, S. R. Marder, P. Miles, T. Wada, M. Tian, H. Sasabe *Science* **1996**, *273*, 1533−1536.
[3] G. K. Lim, Z. L. Chen, J. Clark, R. G. S. Goh, W. H. Ng, H. W. Tan, R. H. Friend, P. K. H. Ho, L. L. Chua, *Nat. Photon.* **2011**, *5*, 554−560.
[4] J. Shirk, R. G. S. Pong, F. J. Bartoli, A. W. Snow, *Appl. Phys. Lett.* **1993**, *63*, 1880−1882.
[5] J. W. Perry, K. Mansour, S. R. Marder, K. J. Perry, D. Alvarez Jr., I. Choong, *Opt. Lett.* **1994**, *19*, 625−627.
[6] S. Hughes, G. Spruce, B. S. Wherrett, T. Kobayashi, *J. Appl. Phys.* **1997**, *81*, 5905−5912.
[7] J. S. Shirk, R. G. S. Pong, S. R. Flom, H. Heckmann, M. Hanack, *J. Phys. Chem. A* **2000**, *104*, 1438−1449.
[8] M. Calvete, G. Y. Yang, M. Hanack, *Synth. Met.* **2004**, *141*, 231−243.
[9] Y. Chen, M. Hanack, Y. Araki, O. Ito, *Chem. Soc. Rev.* **2005**, *34*, 517−529.
[10] Y. Chen, M. Hanack, W. J. Blau, D. Dini, Y. Liu, Y. Lin, J. Bai, *J. Mater. Sci.* **2006**, *41*, 2169−2185.
[11] M. O. Senge, M. Fazekas, E. G. A. Notaras, W. J. Blau, M. Zawadzka, O. B. Locos OB, E. M. NiMhuircheartaigh, *Adv. Mater.* **2007**, *19*, 2737−2774.
[12] Q. D. Zheng, S. K. Gupta, G. S. He, L. S. Tan, P. N. Prasad, *Adv. Funct. Mater.* **2008**, *18*, 2770−2779.
[13] D. Dino, M. F. J. Calvete, M. Hanack, *Chem. Rev.* **2016**, *116*, 13043−14276.
[14] Y. P. Sun, J. E. Riggs, H. W. Rollins, R. Guduru, *J. Phys. Chem. B* **1999**, *103*, 77−82.
[15] Y. P. Han, M. H. Luo, Q. W. Wang, J. X. Wang, X. L. Gao*, Adv. Mater. Res.* **2011**, *295*, 152−155.
[16] P. Chen, X. Wu, X. Sun, J. Lin, W. Ji, K. L. Tan, *Phys. Rev. Lett.* **1999**, *82*, 2548−2551.
[17] L. W. Tutt, T. F. Boggess, *Prog. Quant. Electron.* **1993**, *17*, 299−338.
[18] J. Wang, W. J. Blau, *J. Opt. A* **2009**, *11*, 024001.
[19] R. L. Sutherland, *Handbook of Nonlinear Optics*, 2nd ed., Marcel Dekker, New York, **2003**.
[20] E. W. Van Stryland, M. Sheik-Bahae in *Characterization Techniques and Tabulations for Organic Nonlinear Materials*, (Eds. M. G. Kuzyk, C. W. Dirk), Marcel Dekker, New York, **1998**, pp. 655-692.
[21] A. Ortiz, B. Insuasty, M. R. Torres, M. R. Herranz, N. M. A. Herranz, N. Martin, R. Viruela, *Eur. J. Org. Chem.* **2008**, *1*, 99−108.
[22] S. R. Marder, D. N. Beratan, L. T. Cheng, *Science* **1991**, *252*, 103−106.
[23] T. Yogo, Y. Urano, Y. Ishitsuka, F. Maniwa, T. Nagano, *J. Am. Chem. Soc.* **2005**, *127*, 12162−12163.
[24] C. Mkhize, J. Britton, T. Nyokong, *Polyhedron* **2014**, *81*, 607−613.
[25] K. E. Sekhosana, E. Amuhaya, T. Nyokong, *Polyhedron* **2015**, *85*, 347−354.
[26] T. Kololuoma, J. A. I. Oksanen, P. Raerinne, J. T. Rantala, *J. Mater. Res.* **2001**, *16*, 2186−2188.

10.1002/chem.201702503

[27] M. Frenette, M. Hatamimoslehabadi, S. Bellinger-Buckley, S. Laoui, J. La, S. Bag, S. Mallidi, T. Hasan, B. Bouma, C. Yelleswarapu, J. Rochford, *J. Am. Chem. Soc.* **2014**, *136*, 15853−15856.

[28] B. Kulyk, S. Taboukhat, H. Akdas-Kilig, J.-L. Fillaut, Y. Boughaleb, B. Sahraoui, *RSC Adv.* **2016**, *6*, 84854−84859.

[29] M. Zhu, M. Yuan, X. Liu, C. Ouyang, H. Zheng, X. Yin, Z. Zuo, H. Liu, Y. Li, *J. Polym. Sci. A* **2008**, *46*, 7401−7410.

[30] B. Kulyk, S. Taboukhat, H. Akdas-Kilig, J.-L. Fillaut, M. Karpierz, B. Sahraoui, *Dyes Pigments* **2017**, *137*, 507−511.

[31] Q. Zheng, G. S. He, P. N. Prasad, *Chem. Phys. Lett.* **2009**, *475*, 250−255.

[32] P. Bouit, K. Kamada, P. Feneyrou, G. Berginc, L. Toupet, O. Maury, C. Andraud, *Adv. Mater.* **2009**, *21*, 1151−1154.

[33] A. Loudet, K. Burgess, *Chem. Rev.* **2007**, *107*, 4891−4932.

[34] C. Goze, G. Ulrich, M. L. J. Mallon, B. D. Allen, A. Harriman, R. Ziessel, *J. Am. Chem. Soc.* **2006**, *128*, 10231−10239.

[35] G. Ulrich, C. Goze, M. Guardigli, A. Roda, R. Ziessel, *Angew. Chem. Int. Ed.* **2005**, *44*, 3694−3698.

[36] H. Lu, J. Mack, Y. Yang, Z. Shen, *Chem. Soc. Rev.* **2014**, *43*, 4778−4823.

[37] L. J. Jiao, C. J. Yu, T. Uppal, M. M. Liu, Y. Li, Y. Y. Zhou, E. H. Hao, X. K. Hu, M. G. H. Vicente, *Org. Biol. Chem.* **2010**, *8*, 2517−2519.

[38] M. Sheik-Bahae, A. A. Said, T.-H. Wei, D. J. Hagan, E. W. Van Stryland, *IEEE, J. Quantum Electron.* **1990**, *26*, 760−769.

[39] G. Tsigaridas, I. Polyzos, P. Persephonis, V. A. Giannetas, *Opt. Commun.* **2006**, *266*, 284−289.

[40] J. W. Perry in *Nonlinear Optics of Organic Molecules and Polymers*, (Eds. H. S. Nalwa, S. Miyata), CRC Press, Boca Raton, **1996**.

[41] E. García-Frutos, S. O'Flaherty, E. Maya, G. de la Torre, W. Blau, P. Vázqueza, T. Torres, *J. Mater. Chem.* **2003**, *13*, 749−753.

[42] R. Matthes, *Int. Comm. Health Phys.* **2000**, *79*, 431−440.

[43] R. Hollins, Curr. Opin. *Solid State Mater. Sci.* **1999**, *4*, 189−196.

[44] G. de la Torre, P. Vázquez, F. Agulló-López, T. Torres, *Chem. Rev.* **2004**, **104**, 3723−3750.

[45] B. E. A. Saleh, M. C. Teich, *Fundamentals of Photonics*, Wiley, New York, **1991**.

[46] J. Britton, C. Litwinski, E. Antunes, M. Durmus, V. Chaukea, T. Nyokong, *J. Macromol. Sci. A* **2013**, *50*, 110−120.

[47] D. Dini, M. Hanack in *The Porphyrin Handbook*, Vol. 17, (Eds.: K. M. Kadish, K. M. Smith, R. Guilard), Academic Press, USA, **2003**; pp. 22−31

[48] Y. Wu, X. Mao, X. Ma, X. Huang, Y. Cheng, C. Zhu, *Macromol. Chem. Phys.* **2012**, *213*, 2238−2245.

[49] J. M. Tobin, J. Liu, H. Hayes, M. Demleitner, D. Ellis, V. Arrighi, Z. Xu, F. Vilela, *Polym. Chem.* **2016**, *7*, 6662−6670.

[50] D. Zhang, Y. Wen, Y. Xiao, G. Yu, Y. Liu, X. Qian, *Chem. Commun.* **2008**, 4777−4779.

[51] N. Inoue, Y. Suzuki, K. Yokoyama, I. Karube, *Biosci. Biotechnol. Biochem.* **2009**, *73*, 1215−1218.

Entry for the Table of Contents

FULL PAPER

BODIPYs as optical limiters: The optical limiting properties of a series of 3,5-dithienylenevinylene BODIPY dyes with D-π-A type structures were studied by using the z-scan technique at 532 nm in the nanosecond pulse range. An unusually strong reverse saturable absorption RSA response was observed when the compounds are embedded in poly(bisphenol carbonate A) polymer thin films.

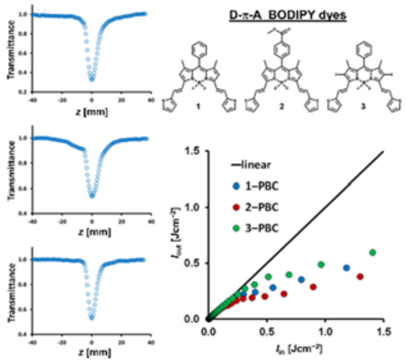

Jessica Harris, Lizhi Gai, Gugu Kubheka, John Mack, Tebello Nyokong and Zhen Shen**

Page No. – Page No.

Optical limiting properties of 3,5-dithienylenevinylene BODIPY dyes at 532 nm